Supporting Information

Monoclinic $SrIrO_3$: an easily-synthesized conductive perovskite oxide with outstanding performance for overall water splitting in alkaline solution

Jie Yu, Xinhao Wu, Daqin Guan, Zhiwei Hu, Shih-Chang Weng, Hainan Sun, Yufei Song, Ran Ran, Wei Zhou, Meng Ni and Zongping Shao**

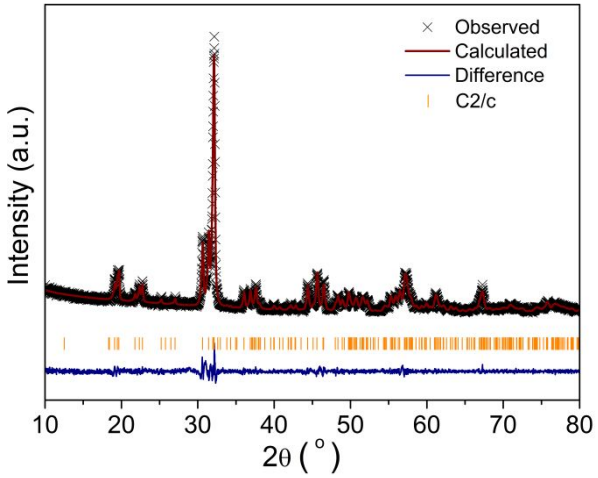

Figure S1. Rietveld refinement results of the XRD pattern of the as-synthesized perovskite $SrIrO_3$.

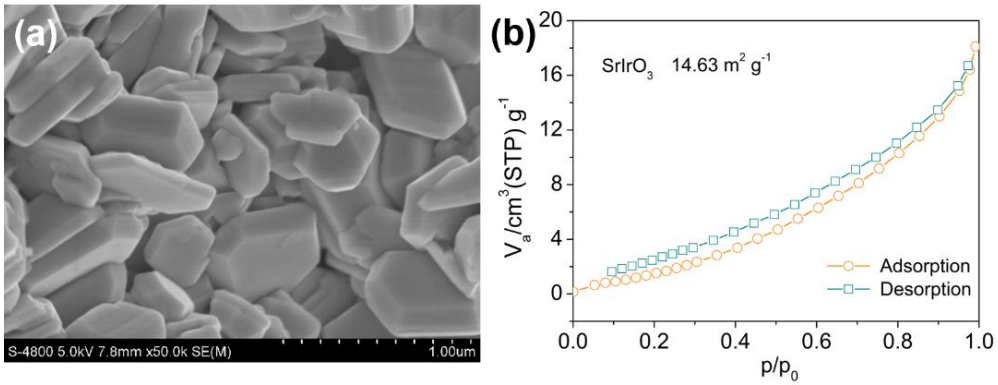

Figure S2. (a) SEM image and (b) Nitrogen adsorption-desorption isotherm curves of the as-synthesized $SrIrO_3$.

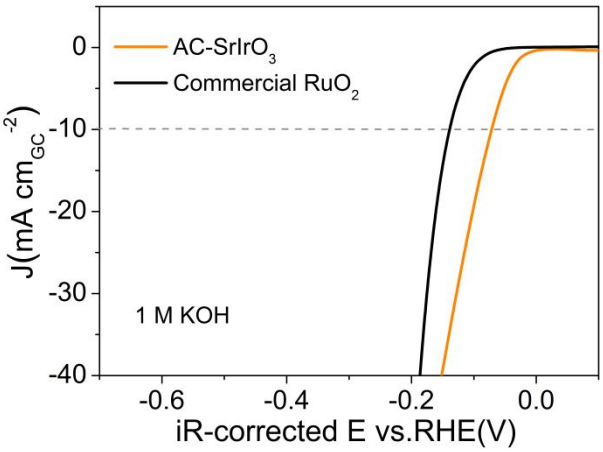

Figure S3. Typical HER polarization curve of the AC-$SrIrO_3$ and commercial RuO_2 samples

in Ar-saturated 1 M KOH solution.

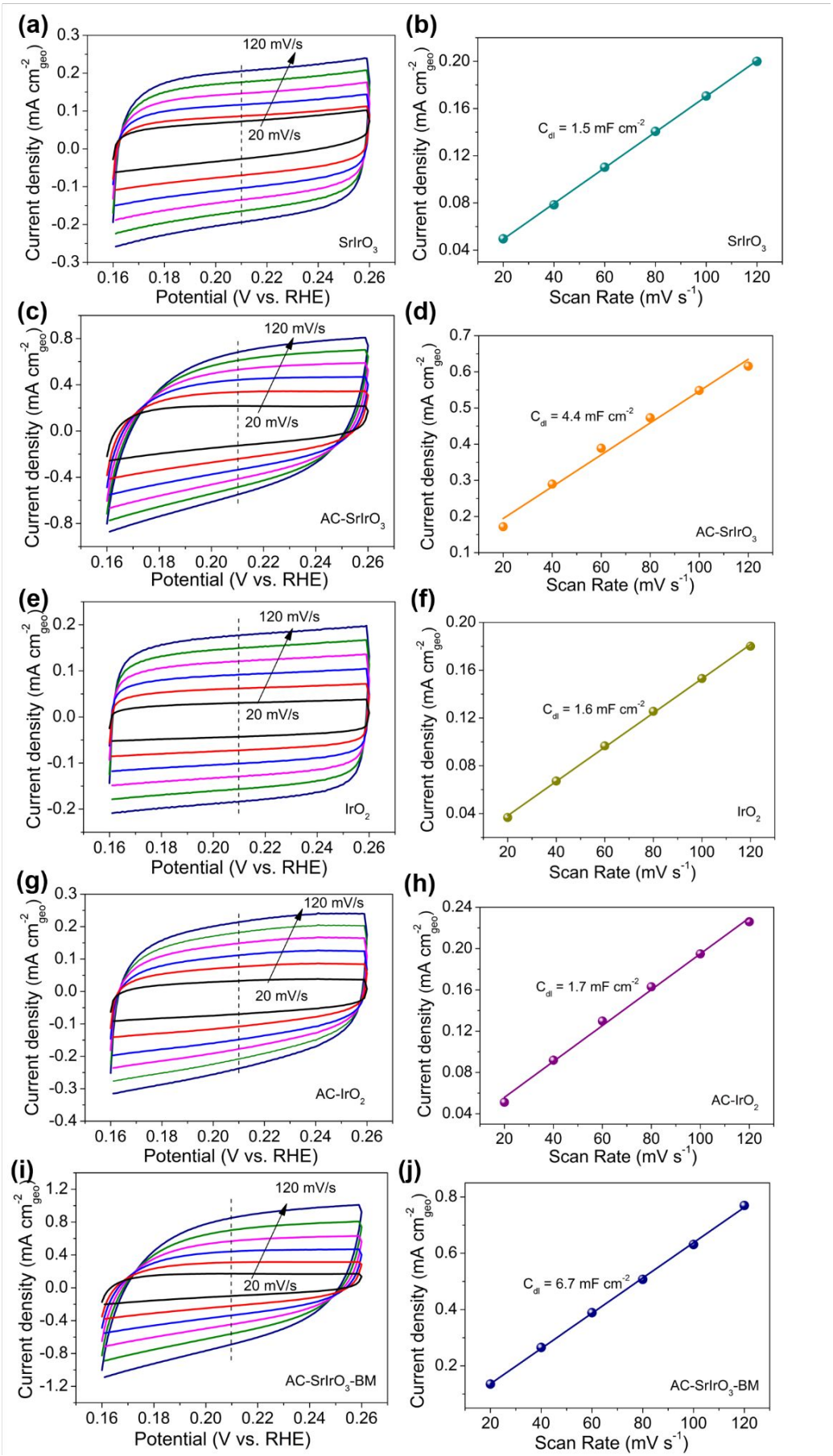

Figure S4. Cyclic voltammetry profiles at different scan rates (20-120 mV s^{-1}) and linear fitting

curve (capacitive currents vs. CV scan rates) for $SrIrO_3$ (a, b), AC-$SrIrO_3$ (c, d), IrO_2 (e, f), AC-IrO_2 (g, h) and AC-$SrIrO_3$-BM (i, j) samples in 0.1 M KOH.

The ECSA of these oxides is calculated from the following formula, whereas the specific capacitance (Cs) is 0.04 mF cm^{-2} in 0.1 M KOH electrolytes:[1-3] $ECSA = C_{dl}/(Cs \times m_{catalyst})$. As to Pt/C, previous study has demonstrated that the obtained ECSA was 71 m^2 g^{-1} in 0.1 M KOH.[4]

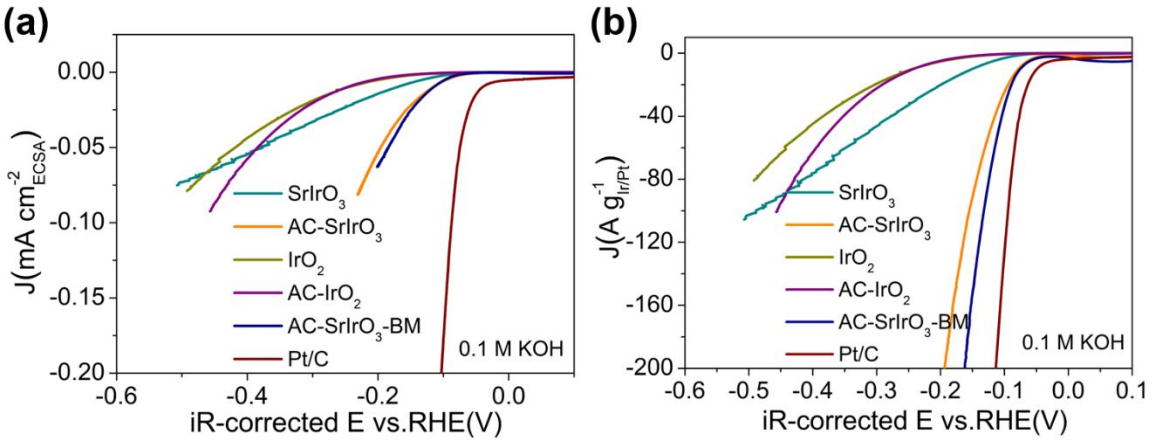

Figure S5. (a) Specific activity (SA) and (b) mass activity (MA) of $SrIrO_3$, AC-$SrIrO_3$, IrO_2, AC-IrO_2, AC-$SrIrO_3$-BM and commercial Pt/C by being normalized to their corresponding ECSA and noble metal mass, respectively.

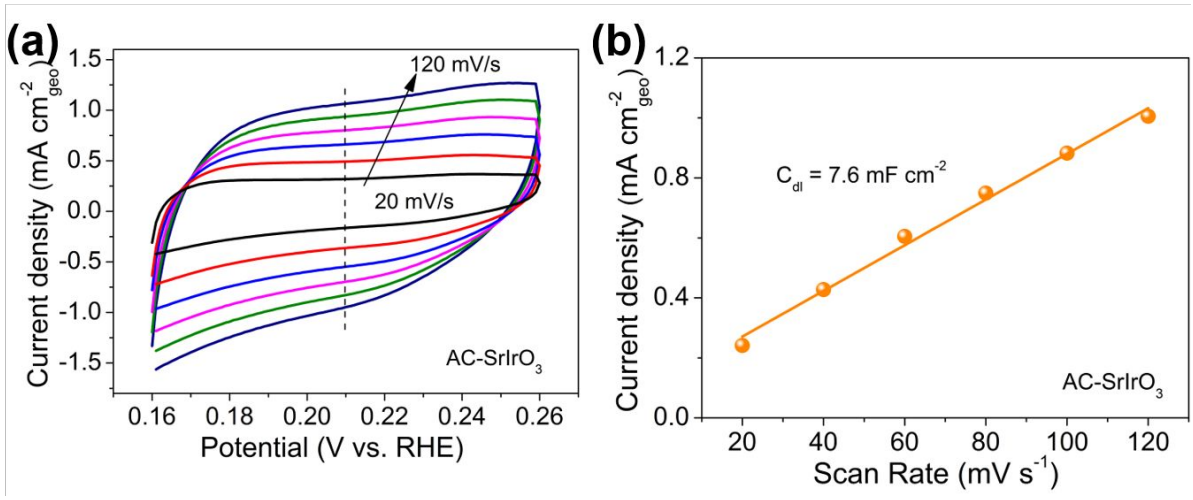

Figure S6. (a) Cyclic voltammetry profiles at different scan rates (20-120 mV s^{-1}) and (b) linear fitting curve (capacitive currents vs. CV scan rates) for AC-$SrIrO_3$ in 1 M KOH.

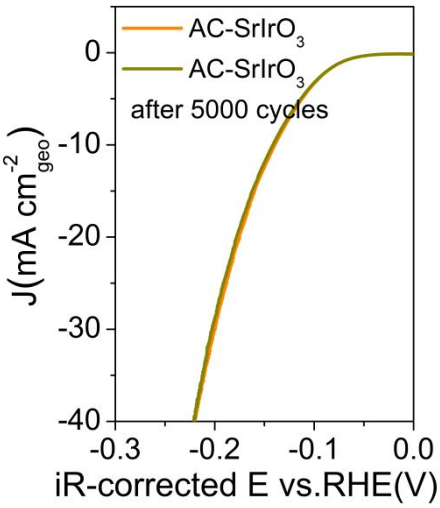

Figure S7. HER polarization curves of AC-$SrIrO_3$ sample initially and after 5000 cycles.

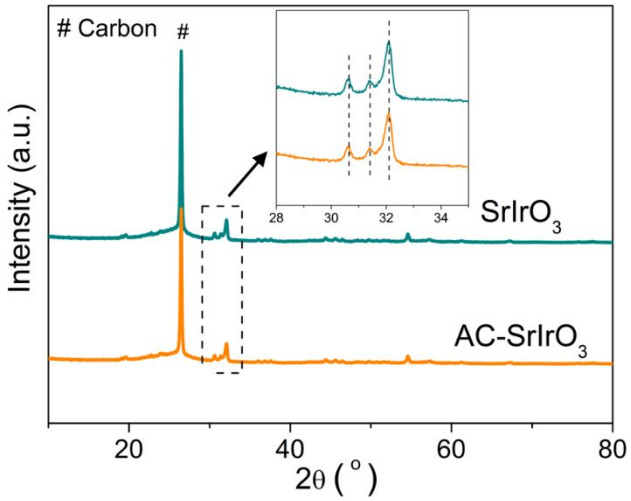

Figure S8. Typical XRD patterns of $SrIrO_3$ and AC-$SrIrO_3$ samples supported on the carbon paper substrate. The insert is a magnified XRD pattern, which displayed dominant peaks of the monoclinic $SrIrO_3$ phase.

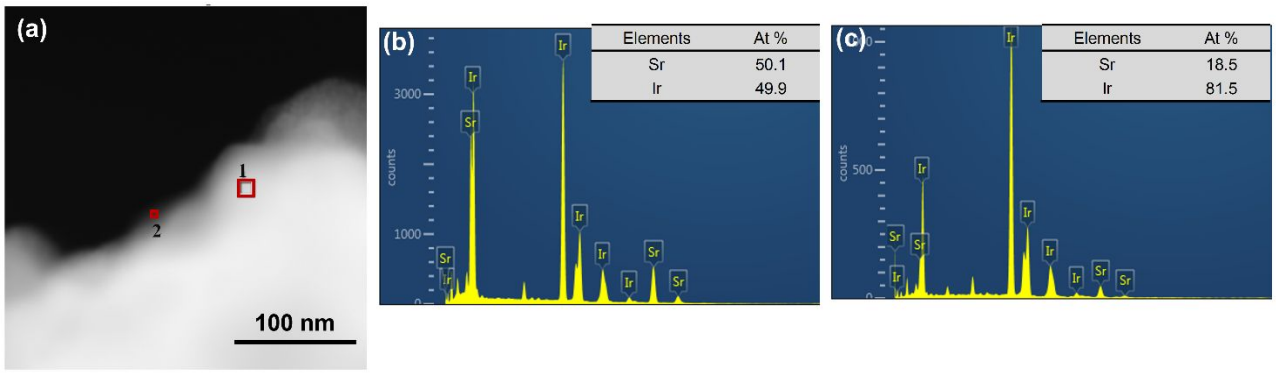

Figure S9. (a) High-angle annular dark-field scanning TEM image of AC-$SrIrO_3$. (b, c) EDX spectra of AC-$SrIrO_3$ measured at position 1 (a) and 2 (b) in Figure S9a.

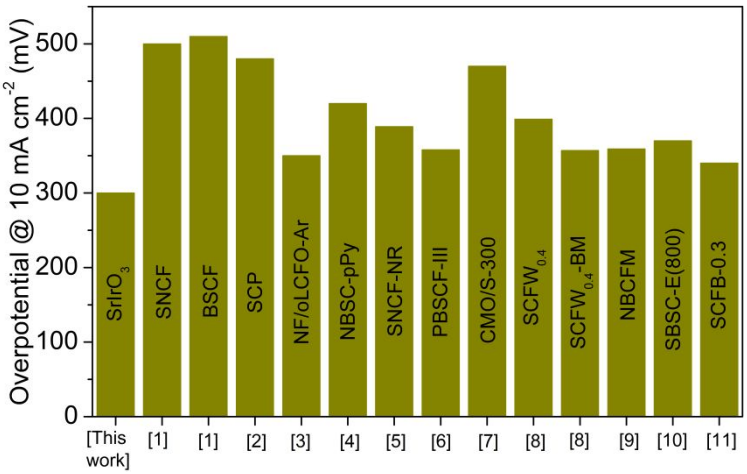

Figure S10. OER activity comparison of $SrIrO_3$ in this work with the state-of-the-art perovskite oxides reported elsewhere. The electrolyte was 0.1 M KOH. Ref [1]-[11] can be obtained from Table S5.

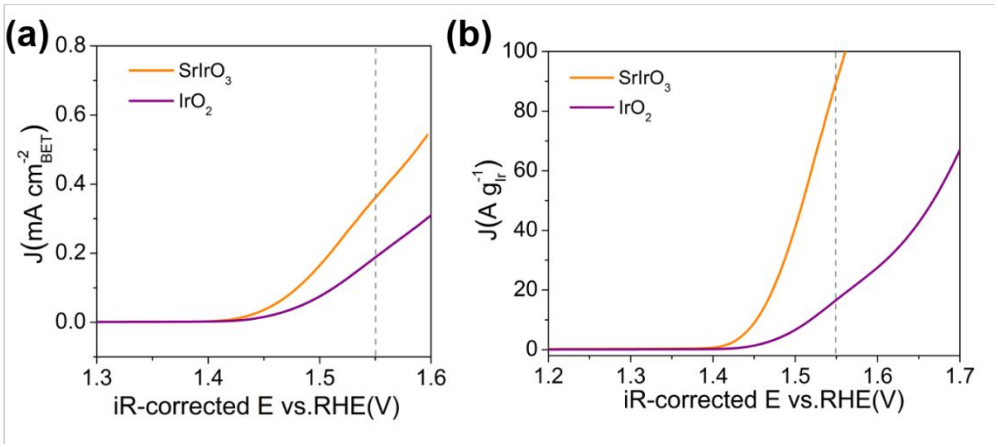

Figure S11. (a) SA and (b) MA of $SrIrO_3$ and IrO_2 toward OER by being normalized to their corresponding BET surface areas and noble metal mass, respectively.

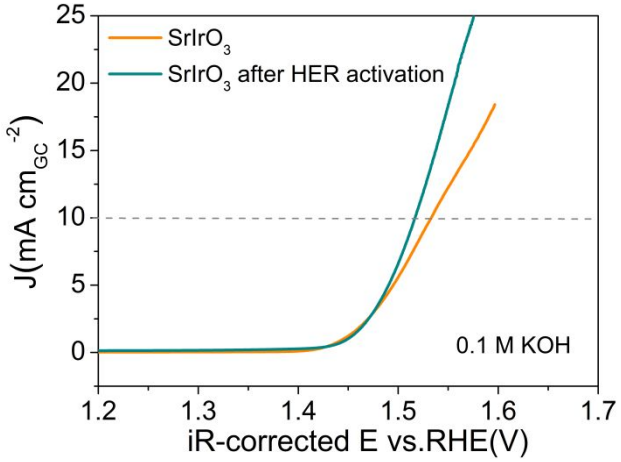

Figure S12. OER polarization curves of $SrIrO_3$ and $SrIrO_3$ after HER activation in the O_2-saturated 0.1 M KOH electrolytes.

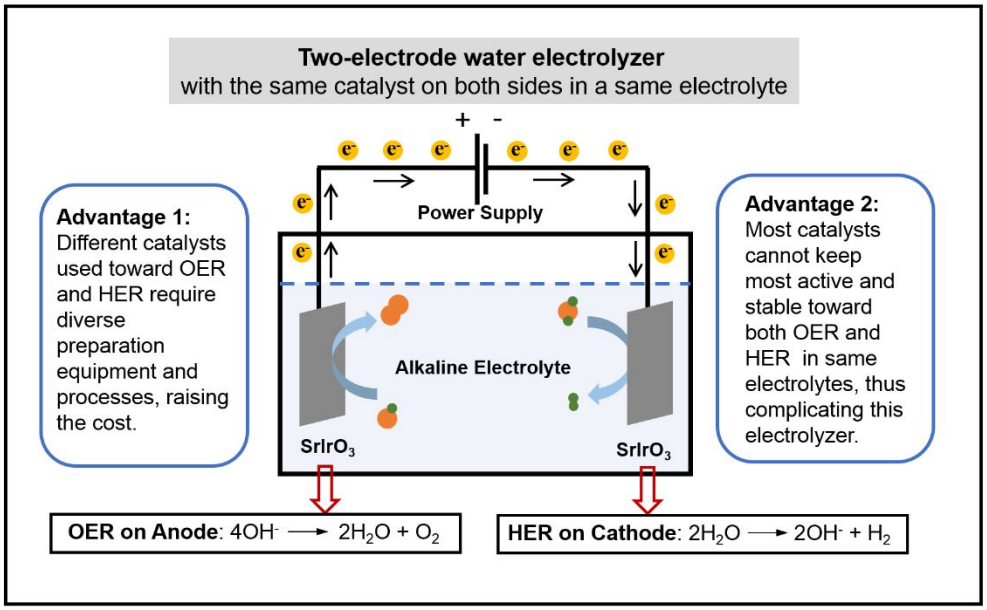

Figure S13. Schematic diagram of a two-electrode water electrolyzer with the same catalyst at both electrodes, which outlined the advantages of such a design.

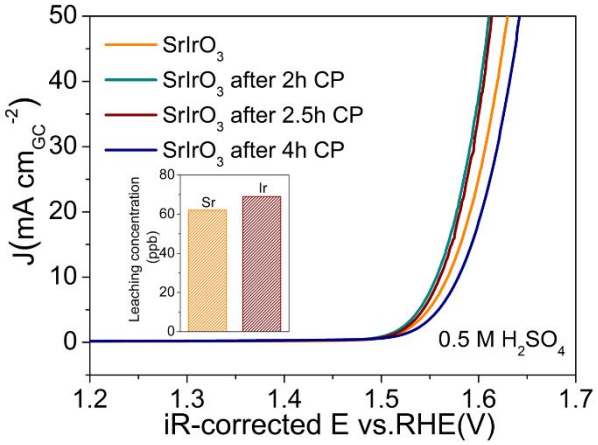

Figure S14. LSV measurements from $SrIrO_3$ during the different time of chronopotentiometric (CP) testing at a fixed current density of 10 mA cm^{-2}_{GC}. Inset: the leaching concentration of Sr and Ir in $SrIrO_3$ after a stability testing.

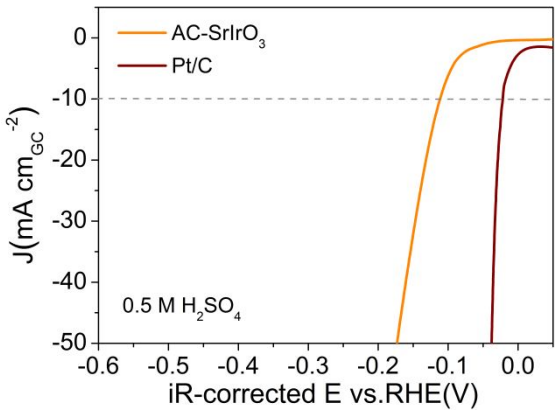

Figure S15. LSV curves toward HER of AC-$SrIrO_3$, and benchmark Pt/C samples in Ar-saturated 0.5 M H_2SO_4 electrolytes.

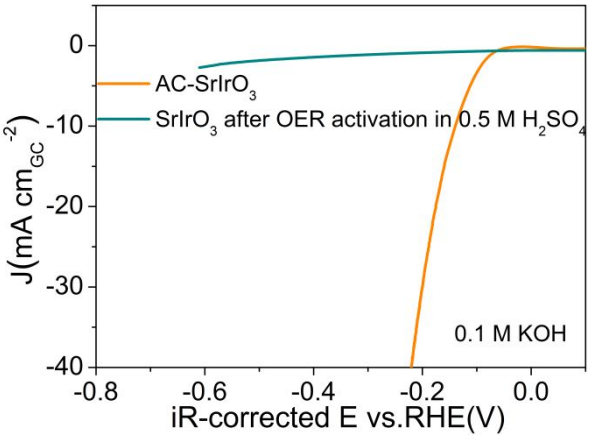

Figure S16. HER polarization curves in the alkaline media for the AC-$SrIrO_3$ electrode and the $SrIrO_3$ electrode after the activation under acidic OER condition in acidic condition.

Table S1. Refined structure information of $SrIrO_3$.

	$SrIrO_3$
Space group	Monoclinic (C2/c)
Perovskite (wt. %)	100
Lattice parameters	
a (Å)	5.6004(9)
b (Å)	9.6205(8)
c (Å)	14.1391(3)
α (°)	90
β (°)	93.10
γ (°)	90
R_{exp}	7.20%
R_{wp}	8.58%
GOF	1.19

Table S2. Specific surface area data of $SrIrO_3$ and IrO_2.

Sample	S_{BET}[a] (m^2 g^{-1})
$SrIrO_3$	14.63
IrO_2	7.62
[a]S_{BET}: specific surface area from BET method.	

Table S3. Comparison of HER activity of AC-$SrIrO_3$ with many reported perovskite oxides loaded on glass carbon (GC) electrode in alkaline electrolytes.

Catalysts	Electrolyte	η_{10} (mV)	Tafel slope (mV dec^{-1})	SA (mA $cm^{-2}{}_{BET/ECSA}$)	MA (A g^{-1})	References
AC-$SrIrO_3$	0.1 M KOH	139	49	0.054 mA $cm^{-2}{}_{ECSA}$ @200 mV	~220 A $g^{-1}{}_{Ir}$ or 129 A $g^{-1}{}_{Catalyst}$ @200 mV	This work
AC-$SrIrO_3$	1 M KOH	72	--	0.067 mA $cm^{-2}{}_{ECSA}$ @200 mV	~479 A $g^{-1}{}_{Ir}$ or 281 A $g^{-1}{}_{Catalyst}$ @200 mV	This work

AC-$SrIrO_3$-BM	0.1 M KOH	121	49	0.057 mA cm^{-2}_{ECSA} @200 mV	~372 A g^{-1}_{Ir} or 218 A $g^{-1}_{Catalyst}$ @200 mV	This work
Pr0.5BSCF	1 M KOH	237	45	~0.57 mA cm^{-2}_{BET} @200 mV	~7.1 A $g^{-1}_{Catalyst}$ @200 mV*	*Adv. Mater.* **2016**, *28*, 6442.
A-PBCCF-H Fbs	1 M KOH	224	42	--	88 A $g^{-1}_{Catalyst}$ @224 mV*	*Nano Energy* **2017**, *32*, 247.
L-0.5/rGO	1 M KOH	144	46	--	33 A $g^{-1}_{Catalyst}$ @144 mV*	*Adv. Energy Mater.* **2017**, *7*, 1700666.
SNCF-NR	0.1 M KOH	262	134	--	43 A $g^{-1}_{Catalyst}$ @262 mV*	*Adv. Energy Mater*. **2017**, 1602122.
$NBM_{5.5}$	1 M KOH	290	87	--	25 A $g^{-1}_{Catalyst}$ @290 mV*	*ACS Catal.* **2018**, *8*, 364.
e-LSTN	0.1 M KOH	> 400	97	--	--	*J. Mater. Chem. A* **2018**, *6*, 13582.
PBC-1100	0.1 M KOH	245	89	10.23 mA cm^{-2}_{BET} @314 mV	124 A $g^{-1}_{Catalyst}$ @314 mV	*J. Power Sources* **2019**, *427*, 194.
SCFM0.05	1 M KOH	323	94	--	--	*Electrochim. Acta* **2019**, *312*, 128.
Gd0.5	1 M KOH	185	28	4~5 mA cm^{-2}_{BET} @200 mV	11.5~14.4 A $g^{-1}_{Catalyst}$ @200 mV*	*Adv. Funct. Mater.* **2019**, *29*, 1900704
$SrRuO_3$	1 M KOH	101	67	~0.16 mA cm^{-2}_{ECSA} or 2 mA cm^{-2}_{BET} @100 mV	~100 A g^{-1}_{Ru} @100 mV	*Nat. Commun.* **2019**, *10*, 149.

Table S4. Comparison of HER activity of AC-$SrIrO_3$ with several other types of representative materials as reported in literatures.

Catalysts	Electrolyte	η_{10} (mV)	Tafel slope (mV dec^{-1})	SA (mA $cm^{-2}_{BET/ECSA}$)	MA (A g^{-1})	References
AC-$SrIrO_3$	0.1 M KOH	139	49	0.054 mA cm^{-2}_{ECSA} @200 mV	~220 A g^{-1}_{Ir} or 129 A $g^{-1}_{Catalyst}$ @200 mV	This work
AC-$SrIrO_3$	1 M KOH	72	--	0.067 mA cm^{-2}_{ECSA} @200 mV	~479 A g^{-1}_{Ir} or 281 A $g^{-1}_{Catalyst}$ @200 mV	This work
AC-$SrIrO_3$-BM	0.1 M KOH	121	49	0.057 mA cm^{-2}_{ECSA} @200 mV	~372 A g^{-1}_{Ir} or 218 A $g^{-1}_{Catalyst}$ @200 mV	This work

CoP/CC	1 M KOH	209	129	--	~11 A $g^{-1}_{Catalyst}$ @209 mV*	*J. Am. Chem. Soc.* **2014**, *136*, 7587.
Ni@NC	0.1 M KOH	190	--	--	25 A $g^{-1}_{Catalyst}$ @190 mV*	*Adv. Energy Mater.* **2015**, *5*, 1401660.
MoC_x	1 M KOH	151	59	--	12.5 A $g^{-1}_{Catalyst}$ @151 mV*	*Nat. Commun.* **2015**, *6*, 6512.
Mn_1N_1	0.1 M KOH	360	--	--	--	*Adv. Funct. Mater.* **2015**, *25*, 393.
NiMoN	1 M KOH	109	95	--	6.7 A $g^{-1}_{Catalyst}$ @109 mV*	*Adv. Energy Mater.* **2016**, *6*, 1600221.
MPSA/GO-1000	0.1 M KOH	~450	--	--	--	*Angew. Chem. Int. Ed.* **2016**, *55*, 223.
2D-MoS_2/$Ni(OH)_2$-10	0.1 M KOH	240	--	--	--	Adv. Mater. **2018**, *30*, 1801171.
	1 M KOH	185	73	~0.12 mA cm^{-2}_{ECSA} @200 mV	~60.6 A $g^{-1}_{Catalyst}$ @200 mV*	
Bi-NP $Cu_{12}Ni_1Al_{2.6}$	0.1 M KOH	139	110	0.0086 mA cm^{-2}_{ECSA} @200 mV	--	*Adv. Funct. Mater.* **2018**, *28*, 1706127.
Ru/$Y(OH)_3$ NHs	0.1 M KOH	100	66	5 mA cm^{-2}_{ECSA} @~200 mV	--	*Chem. Commun.* **2018**, *54*, 12202.
$Er_2Si_2O_7$:IrO_{2-5}	1 M KOH	170	59	--	--	*ACS Catal.* **2018**, *8*, 8830.

Table S5. Comparison of OER activity of $SrIrO_3$ with various typical active OER catalysts reported so far.

Catalysts	Electrolyte	η_{10} (mV)	Tafel slope (mV dec^{-1})	SA (mA $cm^{-2}_{BET/ECSA}$)	MA (A g^{-1})	References
AC-$SrIrO_3$	0.1 M KOH	300	42	0.36mA cm^{-2}_{BET} @ 320 mV	~ 90 A g^{-1}_{Ir} or 53 A $g^{-1}_{Catalyst}$ @ 320 mV	This work
SNCF	0.1 M KOH	500	76	~17mA cm^{-2}_{BET} @ 500 mV	~44 A $g^{-1}_{Catalyst}$ @ 500 mV	*Angew. Chem. Int. Ed.* **2015**, *54*, 3897.
BSCF	0.1 M KOH	510	94	~10mA cm^{-2}_{BET} @ 500 mV	~39 A $g^{-1}_{Catalyst}$ @ 500 mV	
$SrIrO_3$(100)p/ $DyScO_3$(110)	0.1 M KOH	~400 at η_1	40	--	--	*J. Mater. Chem. A* **2016**, *4*, 6831
SCP	0.1 M KOH	480	84	--	--	*Adv. Funct. Mater.* **2016**, *26*, 5862.

NF/oLCFO-Ar	0.1 M KOH	350	59		~9 A $g^{-1}_{Catalyst}$ @ 350 mV*	*Sci. Adv.* **2016**, *2*, e1600495.
NBSC-pPy	0.1 M KOH	420	--	--	--	*Energy Environ. Sci.* **2017**, *10*, 523.
SNCF-NR	0.1 M KOH	389	61	--	~43 A $g^{-1}_{Catalyst}$ @ 389 mV*	*Adv. Energy Mater.* **2017**, *7*, 1602122.
$NBM_{5.5}$	1 M KOH	430	75	2.06 mA cm^{-2}_{BET} @470 mV	107 A $g^{-1}_{Catalyst}$ @470 mV	*ACS Catal.* **2018**, *8*, 364.
PBSCF-III	0.1 M KOH	358	52	~3.8 mA cm^{-2}_{BET} @370 mV	~70 A $g^{-1}_{Catalyst}$ @370 mV	*Nat. Commun.* **2017**, *8*, 14586.
CMO/S-300	0.1 M KOH	470	--	--	--	*Adv. Energy Mater.* **2018**, *8*, 1800612.
$SCFW_{0.4}$	0.1 M KOH	399	50	~2.1 mA cm^{-2}_{BET} @410 mV	~60 A $g^{-1}_{Catalyst}$ @410 mV	*J. Mater. Chem. A* **2018**, *6*, 9854.
$SCFW_{0.4}$-BM		357	58	~1.9 mA cm^{-2}_{BET} @410 mV	~140 A $g^{-1}_{Catalyst}$ @410 mV	
NBCFM	0.1 M KOH	359	81	--	--	*Sci. Adv.* **2018**, *4*, eaap9360.
SBSC-E(800)	0.1 M KOH	370	46	0.33 mA cm^{-2}_{BET} @370 mV	43.1 A $g^{-1}_{Catalyst}$ @370 mV	*J. Mater. Chem. A,* **2019**, *7*, 19228.
SCFB-0.3	0.1 M KOH	340	58	7.6 mA cm^{-2}_{BET} @350 mV	58.5 A $g^{-1}_{Catalyst}$ @350 mV	*Adv. Energy Mater.* **2019**, *9*, 1900429.
20 wt% Ir/C	0.1 M KOH	380	--	--	--	*J. Am. Chem. Soc.* **2010**, *132*, 13612.
20 wt% Ru/C	0.1 M KOH	390	--	--	--	
CoCo LDH	1 M KOH	393	59	--	--	*Nat. Commun*. **2014**, *5*, 4477.
Surface-clean 3D Ir	0.1 M KOH	296	42	--	--	*Nano letters* **2016**, *16*, 4424.
$Ni_{0.9}Fe_{0.1}PS_3$	1 M KOH	329	69	--	--	*ACS Catal.* **2017**, *7*, 8549.
$Ir_{0.71}Cu_{0.29}$	1 M NaOH	335	--	--	~112 A g^{-1}_{Ir} @ 335 mV*	*Angew. Chem. Int. Ed.* **2018**, *57*, 4505.
$NiCo_2S_4$@g-C_3N_4-CNT	1 M KOH	330	57	--	--	*Adv. Mater.* **2019**, *31*, 1808281.

Table S6. Summary of overall-water-splitting performance of some recently well-developed bifunctional electrocatalysts in a 1M KOH solution.

Catalysts (Anode-Cathode)	Substrate	Loading (mg cm^{-2}_{geo})	Current density (mA cm^{-2}_{geo})	Potential (V)	MA (A $g^{-1}_{Catalyst}$)*	References
$SrIrO_3$-AC-$SrIrO_3$	Carbon cloth	5	10	1.59	2@360 mV	This work
SNCF-NR	Ni foam	3	10	1.68	3.3@450 mV	*Adv. Energy Mater.* **2017**, *7*, 1602122.

L-0.5/rGO	F-doped tin oxide	0.5	50	1.76	100@530 mV	*Adv. Energy Mater.* **2017**, *7*, 1700666.
$NBM_{5.5}$	Ni foam	--	10	1.65	--	*ACS Catal.* **2018**, *8*, 364.
NiFe LDHs	Ni foam	--	10	1.7	--	*Science* **2014**, *345*, 1593.
EG/$Co_{0.85}$Se/Ni Fe-LDH	--	4	10	1.67	2.5@440 mV	*Energy Environ. Sci.* **2016**, *9*, 478.
Ni/NiP	Ni foam	10.58	10	1.61	~1@380mV	*Adv. Funct. Mater.* **2016**, *26*, 3314.
CoP@a-CoOx plate	Carbon cloth	5	10	1.66	2@430 mV	*Adv. Sci.* **2018**, *5*, 1800514

* in all Tables represented that these data was obtained by our calculation

References

(1) Wu, G.; Zheng, X. S.; Cui, P. X.; Jiang, H. Y.; Wang, X. Q.; Qu, Y. T.; Chen, W. X.; Lin, Y.; Li, H.; Han, X.; Hu, Y. M.; Liu, P G.; Zhang, Q. H.; Ge, J. J.; Yao, Y. C.; Sun, R. B.; Wu, Y. E. ; Gu, L.; Hong, X.; Li, Y. D. A General Synthesis Approach for Amorphous Noble Metal Nanosheets. *Nature Commun.* **2019**, *10*, 4855.

(2) Zhang, R.; Wang, X. X.; Yu, S. J.; Wen, T.; Zhu, X. W.; Yang, F. X.; Sun, X. N.; Wang, X. K.; Hu, W. P. Ternary $NiCo_2P_x$ Nanowires as pH-Universal Electrocatalysts for Highly Efficient Hydrogen Evolution Reaction. *Adv. Mater.* **2017**, *29*, 1605502.

(3) Wang, X.; Xu, Y.; Rao, H.; Xu, W.; Chen, H.; Zhang, W.; Kuang, D.; Su, C. Novel Porous Molybdenum Tungsten Phosphide Hybrid Nanosheets on Carbon Cloth for Efficient Hydrogen. *Energy Environ. Sci.* **2016**, *9*, 1468-1475.

(4) Han, X. P.; Chen, F. Y.; Zhang, T. R.; Yang, J. A.; Hu, Y. X.; Chen, J. Hydrogenated Uniform Pt Clusters Supported on Porous $CaMnO_3$ as a Bifunctional Electrocatalyst for Enhanced Oxygen Reduction and Evolution. *Adv. Mater.* **2014**, *26*, 2047-2051.